DEUTSCHES ELEKTRONEN-SYNCHROTRON DESY

DESY SR-74/13
August 1974

Anisotropy in the Optical Transitions from the π and σ Valence Bands of Graphite

by

R. Klucker, M. Skibowski, and W. Steinmann
Sektion Physik der Universität München

2 HAMBURG 52 · NOTKESTIEG 1

To be sure that your preprints are promptly included in the

HIGH ENERGY PHYSICS INDEX ,

send them to the following address (if possible by air mail) :

DESY
Bibliothek
2 Hamburg 52
Notkestieg 1
Germany

Subject classification: 13.1; 20.1; 21.7

Anisotropy in the Optical Transitions from the π and σ Valence Bands of Graphite[≠]

R. Klucker[+], M. Skibowski, and W. Steinmann

Sektion Physik der Universität München, München, Germany

The dielectric tensor $\hat{\underline{\varepsilon}}(\omega)$ of pyrolytic graphite, cleaved with its surface perpendicular to the c-axis, has been determined using polarized synchrotron radiation of photon energies 3 eV $\leq \hbar\omega \leq$ 40 eV. For this purpose the reflectivities were measured for nine angles of incidence between 15° and 75°, the electric field vector $\underline{E}$ lying parallel and perpendicular to the plane of incidence. The complex dielectric functions $\hat{\varepsilon}_{\perp}$ and $\hat{\varepsilon}_{\parallel}$ for $\underline{E}$ perpendicular and parallel to the c-axis were obtained by a least squares fit of the measured to the calculated reflectivities. In addition $\hat{\varepsilon}_{\perp}$ was determined independently by a dispersion analysis of the reflectivity at 15° angle of incidence. The results showing strong anistropy over the whole energy range are compared with previous optical data for $\hat{\underline{\varepsilon}}$ and electron energy losses. On the basis of recent two and three dimensional band structure calculation the spectra are attributed to direct interband transitions from the π- and σ-type valence bands to π(σ)- and σ(π)-conduction bands for $\underline{E} \perp c$ ($\underline{E} \parallel c$) respectively.

≠ Work supported by the Deutsche Forschungsgemeinschaft and the Deutsches Elektronen-Synchrotron DESY, Hamburg
The paper is based upon the thesis of R. Klucker, University of München, 1972

+ now with Scientific Control System GmbH (SCS), Hamburg 60, Germany

to be published in phys.stat.sol.(b)

Der dielektrische Tensor $\underline{\underline{\hat{\varepsilon}}}(\omega)$ *von pyrolytischem Graphit mit einer Spaltfläche senkrecht zur c-Achse wurde für Photonenenergien zwischen 3 und 40 eV mit polarisierter Synchrotronstrahlung bestimmt. Dazu wurden die Reflektivitäten für neun Einfallswinkel zwischen* 15^{o} *und* 75^{o} *mit dem elektrischen Feldvektor* $\underline{E}$ *parallel und senkrecht zur Einfallsebene gemessen. Die komplexen dielektrischen Funktionen* $\hat{\varepsilon}_{\perp}$ *and* $\hat{\varepsilon}_{\parallel}$ *für* $\underline{E}$ *senkrecht und parallel zur c-Achse wurden aus einem Vergleich von gemessenen und berechneten Reflektivitäten nach der Methode der kleinsten Quadrate erhalten. Unabhängig davon wurde zusätzlich* $\hat{\varepsilon}_{\perp}$ *aus einer Dispersionsanalyse der Reflektivität bei* 15^{o} *Einfallswinkel bestimmt. Die Resultate, die eine starke Anisotropie über den ganzen Energiebereich zeigen, werden mit älteren optischen Daten für* $\underline{\underline{\hat{\varepsilon}}}$ *und Elektronenenergieverlusten verglichen. An Hand neuerer zwei- und dreidimensionaler Bandstrukturberechnungen werden die Spektren direkten Interbandübergängen von* π- *und* σ-*Valenzbändern zu* $\pi(\sigma)$- *und* $\sigma(\pi)$-*Leitungsbändern für* $\underline{E} \perp c$ *(bzw.* $\underline{E} \parallel c$*) zugeordnet.*

1. Introduction

Graphite with its layered structure is a prototype of highly-anisotropic, uniaxial crystals. In first approximation, when interaction between adjacent layers is neglected, graphite can be considered as a two dimensional crystal consisting of interconnected six-atom carbon rings, with its symmetry axis (c-axis) perpendicular to the basal plane. In the tight-binding theory of the electronic states, one distinguishes three σ-bonds per atom (sp^2-hybrids confined to the basal plane) and one π-bond (p_z-orbital perpendicular to the basal plane) being of even and odd parity respectively upon reflection in the basal plane |1|. The anisotropy is expected to manifest itself in optical spectra associated with excitation of valence band electrons, since distinct selection rules govern the transitions between the (bonding) valence band and the (anti-bonding) conduction band |1|. For example, if the electric field vector $\underline{E}$ is polarized perpendicular to the c-axis ($\underline{E} \perp c$) only $\pi \rightarrow \pi^*$ and $\sigma \rightarrow \sigma^*$ transitions are allowed in dipole approximation, whereas for ($\underline{E} \parallel c$) only $\pi \rightarrow \sigma^*$ and $\sigma \rightarrow \pi^*$ transitions can occur. In comparison with the isotropic case, these and other strong selection rules considerably assist the identification of transitions predicted by band structure calculations |1-3|.

In the past the electronic structure of graphite has been elucidated both theoretically, by several band structure calculations |1-3|, and experimentally by investigations of the reflectivity |4-6|, photoemission |7|, secondary electron emission |7|, and electron energy losses |8-10|. The purpose of this work is to extend the optical reflection measurements, with polarized light, beyond the present limit of 5 eV |6| and to determine the full dielectric tensor $\underline{\underline{\varepsilon}}(\omega)$ up to $\hbar\omega = 40$ eV. We shall also check older optical data |5| available only for $\underline{E} \perp c$; for example, we shall compare the old value of the (σ+π) plasmon energy (where $|\mathrm{Im}\varepsilon_{\perp}^{-1}|$ has its maximum)

of 25 eV |5|, with the more precise value 27 eV extracted from our data. The exact values of the plasmon energies are of interest in connection with the maxima recently observed in the energy loss spectra of fast electrons |8,9| and the numerous satellites observed in the appearance potential spectrum of graphite |11|.

In this paper we briefly summarize our experimental results and compare our data with previous results of the optical investigations |5,6| and of electron energy loss spectroscopy |8-10|.

2. Experiment and Results

The reflectance of freshly cleaved samples of pyrolytic graphite (c-axis perpendicular to the surface) has been measured for photon energies between 3 eV and 40 eV at room temperature for angles of incidence between 15° and 75° in steps of 7.5° using a reflectometer described previously |12|. The light was polarized with its dominant electric field component parallel and perpendicular to the plane of incidence. The spectral resolution was better than 6 Å (i.e. 0.2 eV at 20 eV). The intense polarized continuum of the synchrotron radiation of the Deutsches Elektronen-Synchrotron DESY, Hamburg, was used as a light source.

Two types of measurements were performed:

a) "Relative" reflectance measurements: The ratios of the reflectances for the 9 angles between 15° and 75° were determined by measuring the reflected intensities with various types of photomultipliers (an open magnetic multiplier, a Na-salicylate coated multiplier and an uncoated multiplier with quartz window for the different spectral ranges). Both the ordinary and the extraordinary dielectric constants were determined simultaneously (Fig. 1) from the reflectance data by

a modified reflectance-vs-angle-of-incidence method |13|:

For various energies $\hbar\omega$, the weigthed sum Δ (eq. 1) was minimized by varying the five real quantities: the four ordinary and extraordinary dielectric constants $\hat{\varepsilon}_{\perp} = \varepsilon_{1\perp}+i\varepsilon_{2\perp}$, $\hat{\varepsilon}_{\parallel} = \varepsilon_{1\parallel}+i\varepsilon_{2\parallel}$ and the degree of polarization α. ($\alpha = (I_p-I_s)(I_p+I_s)^{-1}$, I_p and I_s being the intensity of the incident light parallel and perpendicular to the synchrotron plane, values for α determined by this procedure always fell within the experimentally acceptable range $0.9<\alpha<0.97$).

$$\Delta = \sum_{p,j,k} \left(S_{pjk}\left(1- \frac{R_{pj}}{R_{pk}} \cdot \frac{r_{pk}}{r_{pj}}\right)^2\right) \qquad (1)$$

with φ_j, φ_k: angles of incidence

p : direction of the polarization (dominant component parallel or perpendicular to the plane of incidence)

$r_{pi}=r_p(\varphi_i)$: measured "relative" reflectance

$R_{pi}=R_p(\varphi_i, \hat{\varepsilon}_{\perp}, \hat{\varepsilon}_{\parallel}, \alpha)$: calculated reflectance using Fresnel's formulas for anisotropic uniaxial crystals (see for instance ref. 14,16)

S_{pjk} : a factor weighting each term of the sum according to its sensitivity in determination of the dielectric constants:

$$S_{pjk} = \sum_x |S_{pjkx}|; \quad S_{pjkx} = \frac{\partial\left(\frac{R_{pj}}{R_{pk}}\right)}{\partial\varepsilon_x} \cdot \frac{\varepsilon_x}{\left(\frac{R_{pj}}{R_{pk}}\right)}; \quad x = 1\perp,\ 2\perp,\ 1\parallel,\ 2\parallel$$

Using the above weighting factors S, an error estimate in the determination of the dielectric constants (shaded area in Fig. 1) was generated. (For details of this procedure see Ref. 16). The energy loss functions $|\mathrm{Im}\hat{\varepsilon}_{\perp}^{-1}|$ and $|\mathrm{Im}\hat{\varepsilon}_{\parallel}^{-1}|$ (Fig. 2), $N_{eff\perp}$ and $N_{eff\parallel}$ (Fig. 3) and the absolute reflectance (Fig. 5) were calculated from the dielectric constants.

b) Absolute reflectance measurements: Absolute reflectivities were obtained by taking the ratio of reflected and incident spectra. A gold-cathode photoelectric diode with good uniform sensitivity minimized errors associated with light spot inversion on the cathode. The absolute reflectance measurements were performed in order to provide a touchstone for comparison with the reflectance values calculated from the dielectric constants obtained by method a). Furthermore the absolute reflectivities obtained for 15° angle of incidence (near normal incidence) were used to determine $\hat{\varepsilon}_{\perp}$ by means of a Kramers-Kronig analysis with appropriate extrapolation |15,16|. The results of this procedure are shown in Fig. 4, and are to be compared with the results in Fig. 1.

Further experimental and computational details are given in Ref. 16.

3. Comparison and Discussion

The gross features of our reflection spectrum for $\underline{E} \perp c$ at 15° angle of incidence generally agree well with those of previous measurements |4-6| and with those derived from electron energy losses |8-10| (Fig. 5, upper half). Major differences in the spectra above 8 eV are the following: The extrapolated values of Taft and Philipp (T) above 25 eV, important for Kramers-Kronig analysis, lie significantly lower than the other two spectra (K,Z). In addition, Zeppenfeld's calculated reflectance |8,9| omits the sharp structure between 15 and 16 eV observed in the optical measurements and also yields markedly smaller absolute values of reflectivity. Obvious differences in magnitude and shape, in particular around 11 eV, are found in the reflection spectra of the various authors for $\underline{E} \parallel c$ (Fig. 5, lower half). All these spectra were obtained by calucations only; we have not measured the reflection for $\underline{E} \parallel c$, because samples cannot be cleaved with the c-axis parallel to the surface. The spectral

features in the imaginary parts of the dielectric constants $\varepsilon_{2\perp}$ and $\varepsilon_{2\parallel}$ (Fig. 6) are closely related to those in the reflection spectra.

The optical and energy-loss determinations of the ordinary dielectric constant $\varepsilon_{2\perp}$ are in fair agreement as far as the gross spectral behaviour is concerned - e.g. the main maxima at 4.6 eV and at 14.0 - 14.5 eV. There are, however, apparent differences in the absolute magnitudes and in some fine structure. - Following other authors, we attribute the large 4.5 eV peak to $\pi \rightarrow \pi^*$ transitions between nearly-parallel bands near the critical point Q ($Q_{2u}^- \rightarrow Q_{2g}^-$) |1-3| (compare Fig. 7). This assignment also agrees with recent calculations of the optical spectrum (including matrix element effects) |3|. The 14.5 eV - maximum is ascribed to flat band transitions between the highest occupied σ-band and the lowest σ-conduction band near Q($Q_{2g}^+ \rightarrow Q_{1u}^+$) |2|.

Significant differences among the results computed from optical and energy loss data are found in the $\varepsilon_{2\parallel}$-spectra: there are marked discrepancies in both the general spectral behavior and the absolute magnitudes below 15 eV (Fig. 6). In particular, no prominent maximum at 11.4 eV with $\varepsilon_2 \sim 10$ is derived from the optical measurements. Although the estimated uncertainty in $\varepsilon_{2\parallel}$ is relatively large for $\hbar\omega \sim 10$ eV (see Fig. 1), owing to uncertainties in the degree of polarization α, nevertheless the energy loss data produce a peak five times larger than our experimental uncertainty. Evidence against a strong transition at 11 eV is also provided by band structure calculations |2| as interpreted in the light of recent secondary electron emission measurements. These indicate that only $\sigma \rightarrow \pi^*$ transitions near $Q_{1u}^+ \rightarrow Q_{2g}^-$ (16.5 eV) |2| should contribute significantly to an absorption peak for E $\parallel$ c at $\hbar\omega \sim 15$ eV. The $\sigma \rightarrow \pi^*$ ($P_3^+ \rightarrow P_3^-$) transition once thought to occur at 13.5 eV |2| is forbidden if the P_3^- state lies below the Fermi energy as derived from the results in |7|. The large values, $\varepsilon_{2\parallel} \sim 3$, determined

from energy losses below 5 eV [9] also seem very doubtful in view of recent $\varepsilon_{2\parallel}$ -calculations [3], which yielded values smaller than 0.7 for the π-band contribution to $\varepsilon_{2\parallel}$.

It is interesting also to compare the various results for the energy loss functions $|\mathrm{Im}\varepsilon^{-1}|$, which also exhibit considerable anisotropy (Figs. 2, 8). As expected from the above discussion, the agreement between the optical results and energy loss data for $\underline{E} \perp c$ is gratifying, whereas it is poor for $\underline{E} \parallel c$ and $\hbar\omega \sim 11$ eV. For $\underline{E} \perp c$ a π-plasmon peak is observed at 7 eV and a $\pi+\sigma$ plasmon peak near 27 eV. In addition, both the position and the shape of our $\pi+\sigma$ plasmon peak (located at 27 eV with a half width of 9 eV), agree much better with the energy loss peak at 27.5 eV than with the position of the maximum of $|\mathrm{Im}\varepsilon_{\perp}^{-1}|$ given by Taft and Philipp (25.5 eV, half width $\sim$5 eV). The latter discrepancy is apparently due to an inappropriate extrapolation of Taft and Philipp's normal-incidence reflection spectrum to energies above 25 eV (in order to perform the Kramers-Kronig analysis) [5]. - For $\underline{E} \parallel c$ the values of $|\mathrm{Im}\varepsilon_{\parallel}^{-1}|$ extracted from the optical measurement and from the energy loss spectrum both show maxima at approximately 19 eV.

In Fig. 9 we have plotted the spectra for $\varepsilon_2\omega^2$ for both directions of polarization. If direct interband transitions wholly determine the optical spectrum, then the shape of $\varepsilon_2\omega^2$ should be compared with calculations of the joint density of states modified by matrix elements [1, 3] . The $\varepsilon_2\omega^2$-spectra like the ε_2- or N_{eff}-spectra show the expected anisotropy over the entire spectrum of energies studied: excitation for $\underline{E} \perp c$ is obviously much more efficient than for $\underline{E} \parallel c$. A unique assignment of the peaks in the spectra (especially above 6 eV) to transition occuring at specific points in the Brillouin zone appears difficult in view of uncertainties in existing

band structures and the transitions possible. However, a calculation of (i) the graphite band structure, (ii) π- and σ-band transition matrix elements, and (iii), most importantly, the resulting absorption spectrum $\varepsilon_{2\parallel}$ in a similar way as has been recently done by Johnson and Dresselhaus [3] for π-bands only below 7 eV, would facilitate the identification of the relevant structures and hopefully would also resolve the problem of the 11 eV-structure in the $\varepsilon_{2\parallel}$-spectrum.

Acknowledgments

We are grateful to the members of the synchrotron radiation group at DESY who have supported this work.

We would like to thank also Drs. G. Harbeke and K. Zeppenfeld for supply of a sample of pyrolytic graphite (from Union Carbide) and for valuable discussions of their experimental results. We also appreciate discussions with Dr. E. Tosatti on his analysis of the energy loss spectra and a critical reading of the manuscript by Drs. J. Dow and E.E. Koch.

References

1. G.F. Bassani and G. Pastori-Parravicini, Nuovo Cimento 50 B, 95 (1967) and references therein
2. G.S. Painter and D.E. Ellis, Phys.Rev. B1, 4747 (1970)
3. L.G. Johnson and G. Dresselhaus, Phys.Rev. B7, 2275 (1973)
4. J.G. Carter, R.H. Huebner, R.N. Hamm, and R.D. Birkhoff, Phys.Rev. 137, A639 (1965)
5. E.A. Taft and H.R. Philipp, Phys.Rev. 138, A197 (1965)
6. D.L. Greenaway, G. Harbeke, F. Bassani, and E. Tosatti, Phys.Rev. 178, 1340 (1969
7. R.F. Willis, B. Feuerbacher, and B. Fitton, Phys.Rev. 4, 2441 (1971)
8. K. Zeppenfeld, Z. Physik 211, 391 (1968)
9. K. Zeppenfeld, Thesis, University of Hamburg, 1969 (unpublished)
10. E. Tosatti and F. Bassani, Nuovo Cimento 65B, 161 (1970)
11. A.M. Bradshaw and D. Menzel, phys.stat.sol. (b) 56, 135 (1973)
12. B. Feuerbacher, M. Skibowski, and R.P. Godwin, Rev.Sci.Instr. 40, 305 (1969)
13. W.R. Hunter, J.Opt.Soc.Am. 55, 1197 (1965)
    B. Feuerbacher, M. Skibowski, R.P. Godwin, and T. Sasaki, J.Opt.Soc.Am. 58, 1434 (1968)
14. see for instance J. Cazaux, Nouv.Rev.d'Optique appliquée 2, 397 (1971)
15. R. Klucker, U. Nielsen, Computer Phys.Comm. 6, 187 (1973)
16. R. Klucker, Thesis, University of München, 1972 (unpublished)

Figure Captions

Fig. 1 Dielectric functions of graphite $\hat{\varepsilon}_{\perp} = \varepsilon_{1\perp} + i\varepsilon_{2\perp}$, $\hat{\varepsilon}_{\parallel} = \varepsilon_{1\parallel} + i\varepsilon_{2\parallel}$ for the electric field vector perpendicular and parallel to the symmetry axis ($\underline{E} \perp \underline{c}$ and $\underline{E} \parallel c$) for transitions from π- and σ-bands obtained by the multi-angle reflection method.

Fig. 2 Energy loss functions $|\mathrm{Im}\hat{\varepsilon}_{\perp}^{-1}|$ and $|\mathrm{Im}\hat{\varepsilon}_{\parallel}^{-1}|$ calculated from the results of Fig. 1.

Fig. 3 Effective number of electrons per atom N_{eff} for both directions of polarization, calculated from the results of Fig. 1.

Fig. 4 Dielectric function of graphite $\hat{\varepsilon}_{\perp} = \varepsilon_{1\perp} + i\varepsilon_{2\perp}$ obtained by Kramers-Kronig analysis from absolute reflectivity measurements at 15° angle of incidence.

Fig. 5 Reflectivity at near normal incidence (15°) K (this work), T(Ref. 5), G(Ref. 6), Z (Ref. 8,9).

Fig. 6 Imaginary part of the dielectric function $\varepsilon_{2\perp}$ and $\varepsilon_{2\parallel}$. K (this work), TP(Ref. 5), G (Ref. 6), Z (Ref. 8,9), TB (Ref. 10).

Fig. 7 Two dimensional band structure of graphite calculated by Painter and Ellis (Ref. 2)

Fig. 8 Energy loss functions $|\mathrm{Im}\hat{\varepsilon}_{\perp}^{-1}|$ and $|\mathrm{Im}\hat{\varepsilon}_{\parallel}^{-1}|$ associated with the data of Fig. 6. K (this work), T (Ref. 5), G (Ref. 6), Z (Ref. 8,9).

Fig. 9 Spectrum of $\varepsilon_2\omega^2$ for both directions of polarization, the arrows indicate the main maxima and shoulders respectively.

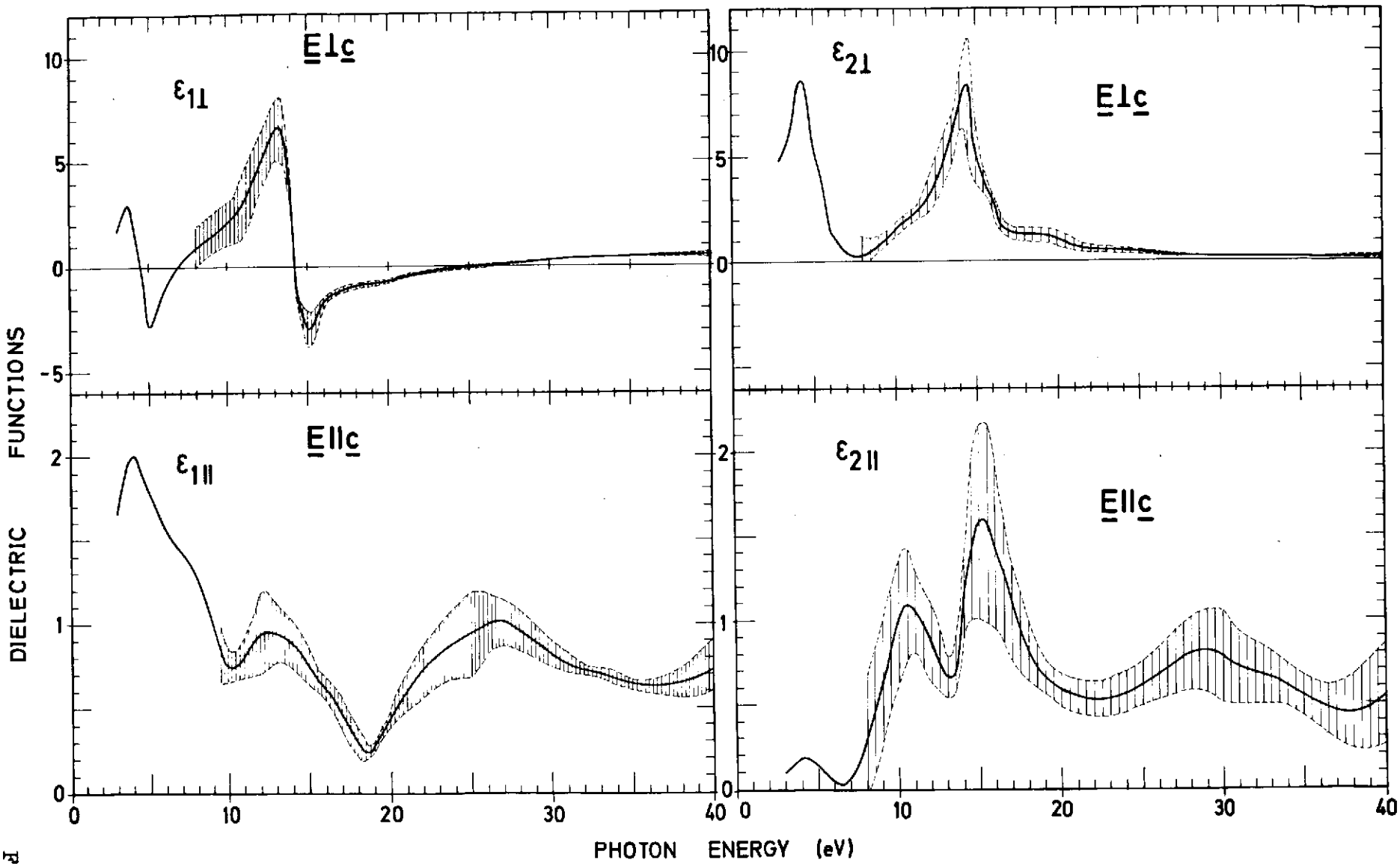
E⊥c
ε1⊥
ε2⊥
E⊥c
E∥c
ε1∥
ε2∥
E∥c
DIELECTRIC FUNCTIONS
PHOTON ENERGY (eV)
10
5
0
-5
2
1
0
10
20
30
40

Fig.1

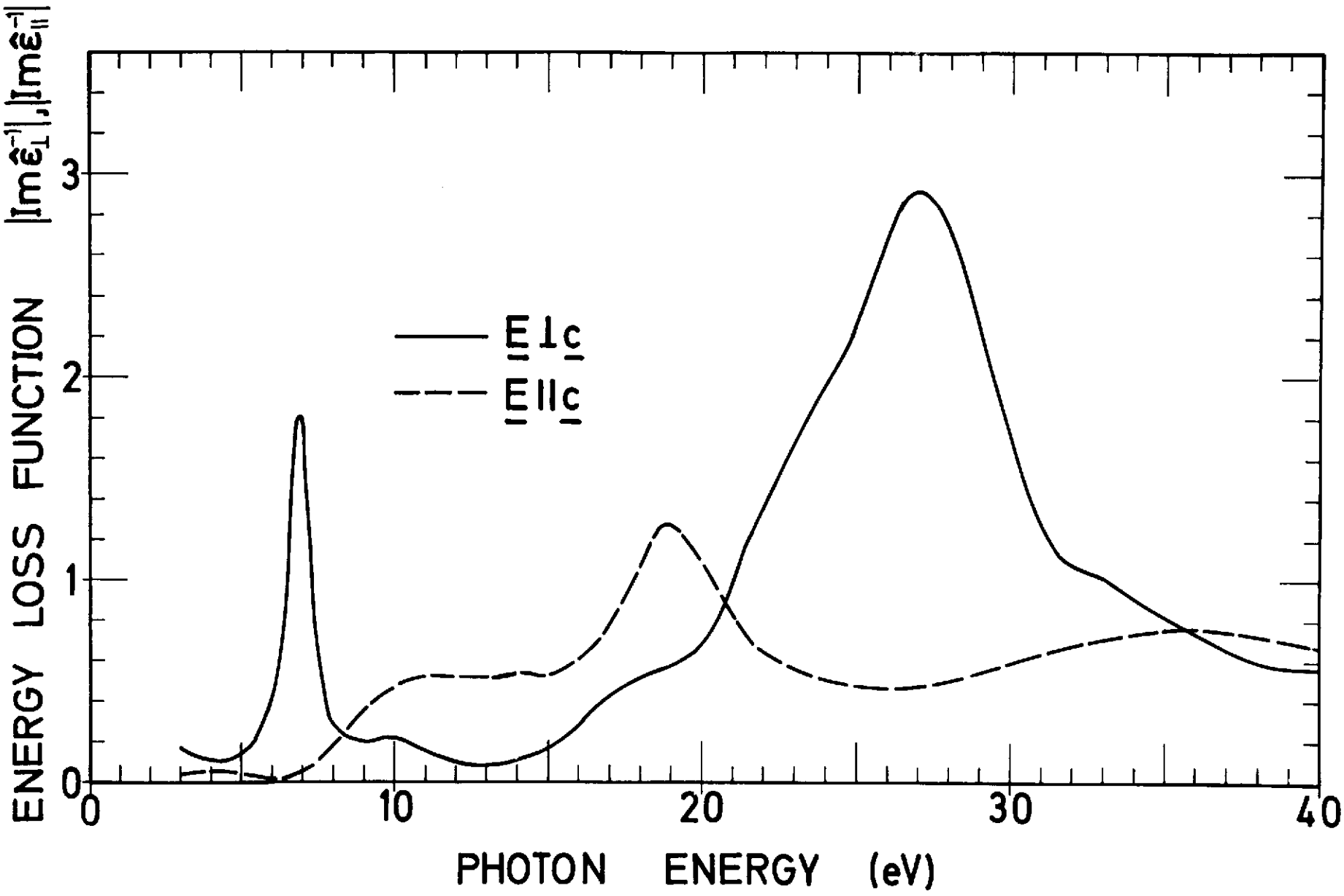
ENERGY LOSS FUNCTION $|Im\hat{\varepsilon}_{\perp}^{-1}|, |Im\hat{\varepsilon}_{\parallel}^{-1}|$
E⊥c
E∥c
0
1
2
3
0
10
20
30
40
PHOTON ENERGY (eV)

Fig. 2

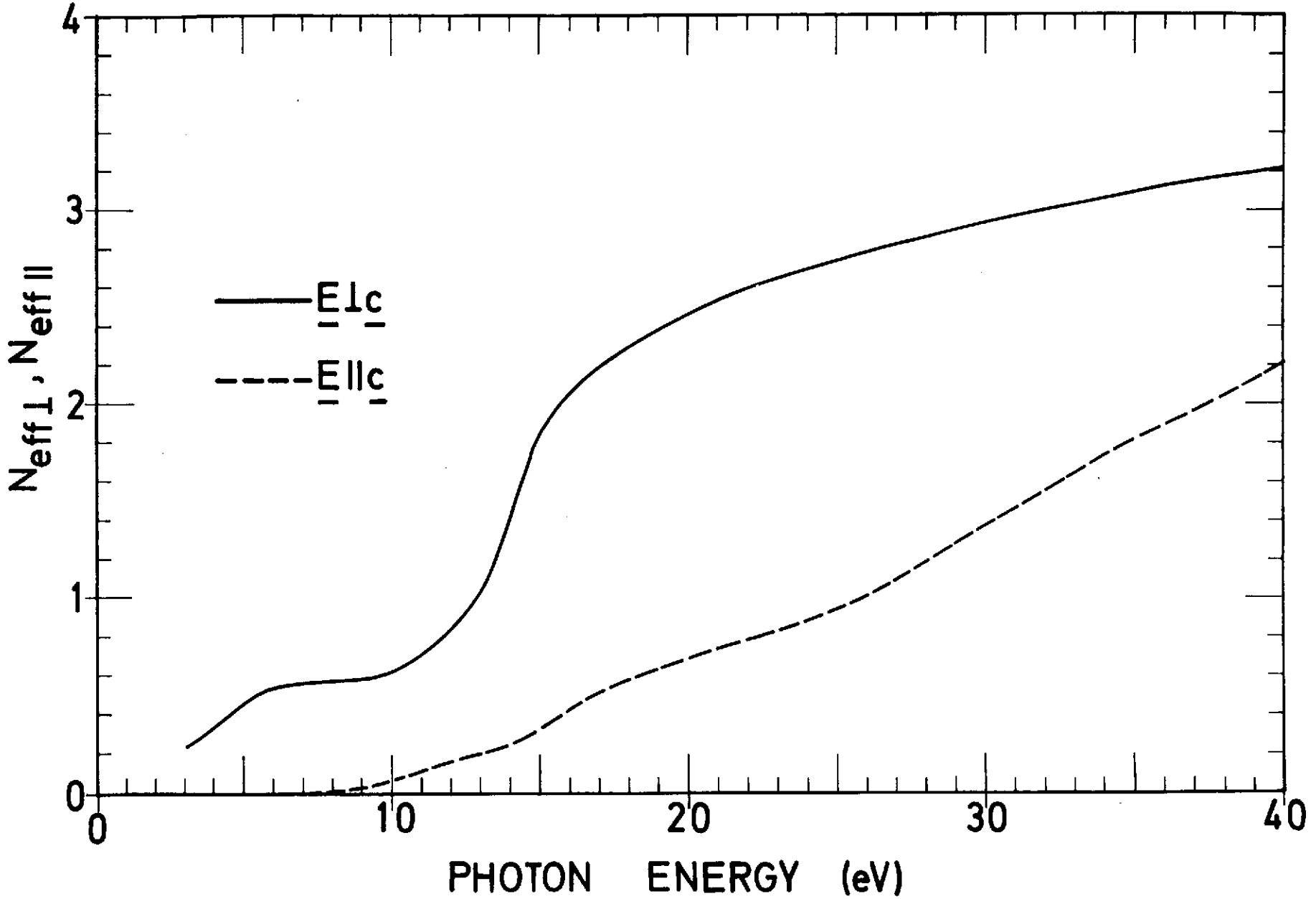
4
3
2
1
0
0
10
20
30
40
$N_{eff\perp}$, $N_{eff\parallel}$
E⊥c
E∥c
PHOTON ENERGY (eV)

Fig. 3

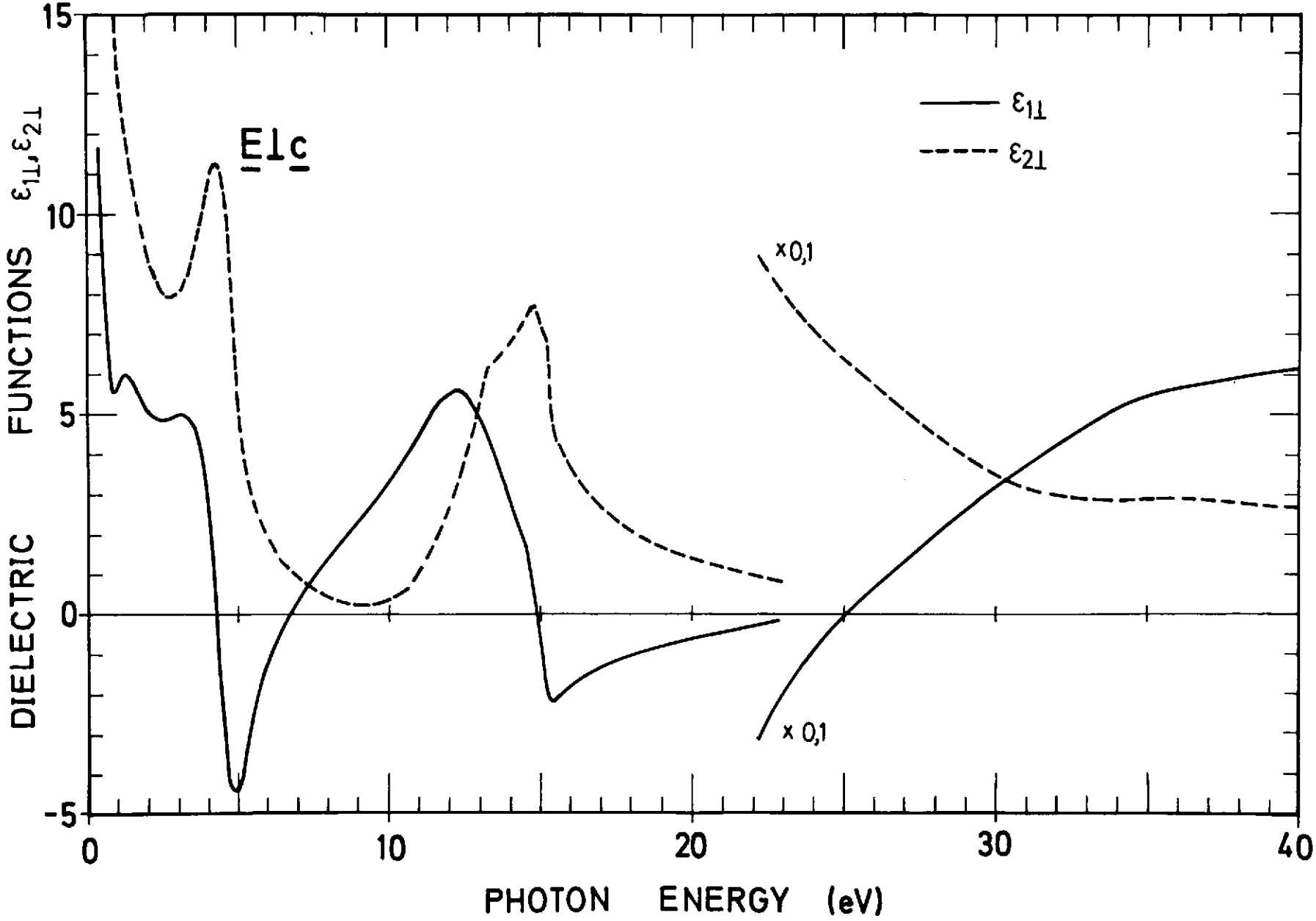
15
10
5
0
-5
0
10
20
30
40
DIELECTRIC FUNCTIONS $\varepsilon_{1\perp}, \varepsilon_{2\perp}$
PHOTON ENERGY (eV)
$\underline{E} \perp \underline{c}$
$\varepsilon_{1\perp}$
$\varepsilon_{2\perp}$
x 0,1
x 0,1

Fig. 4

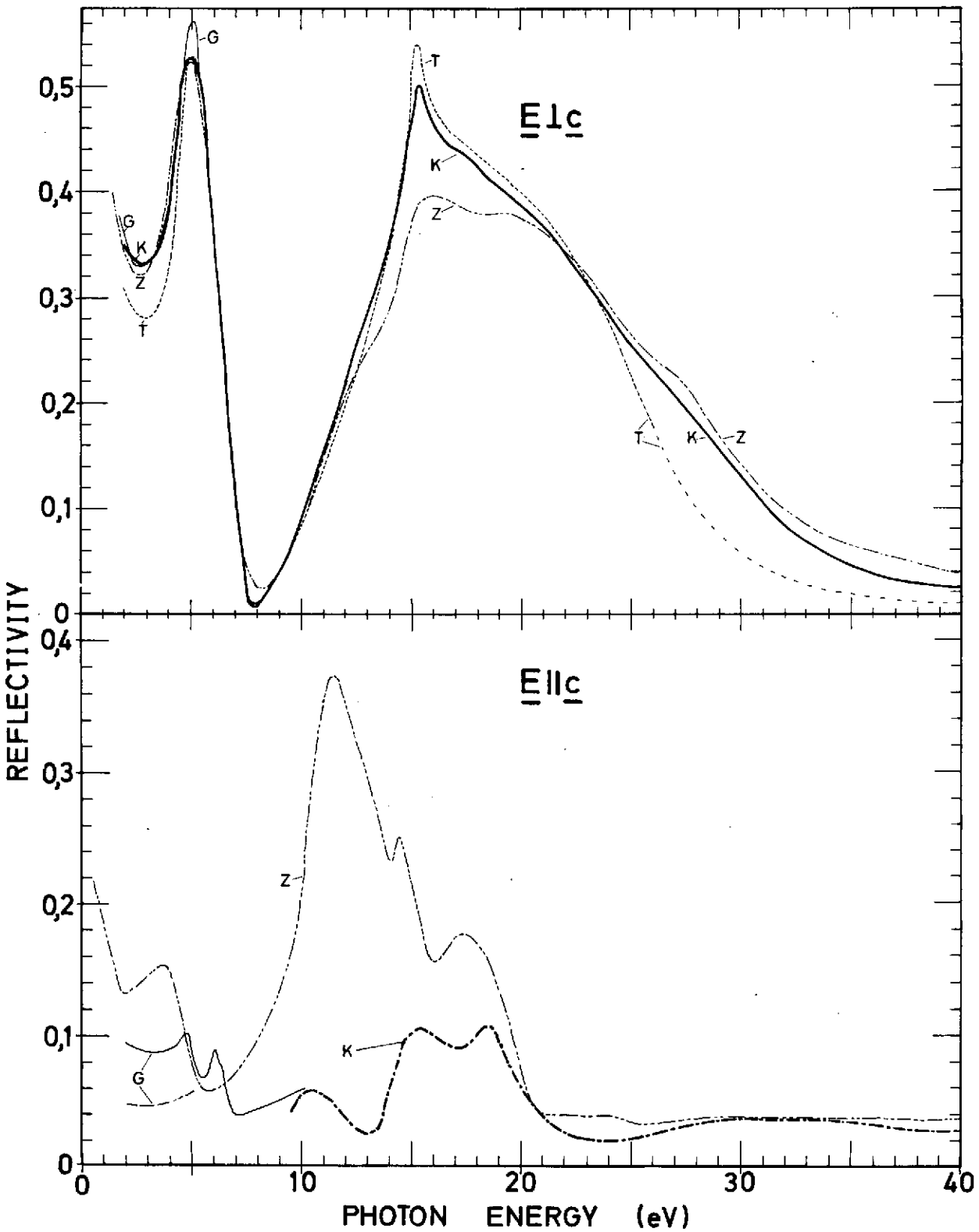
E⊥c
E∥c
G
T
K
Z
REFLECTIVITY
PHOTON ENERGY (eV)
0
0,1
0,2
0,3
0,4
0,5
10
20
30
40

Fig. 5

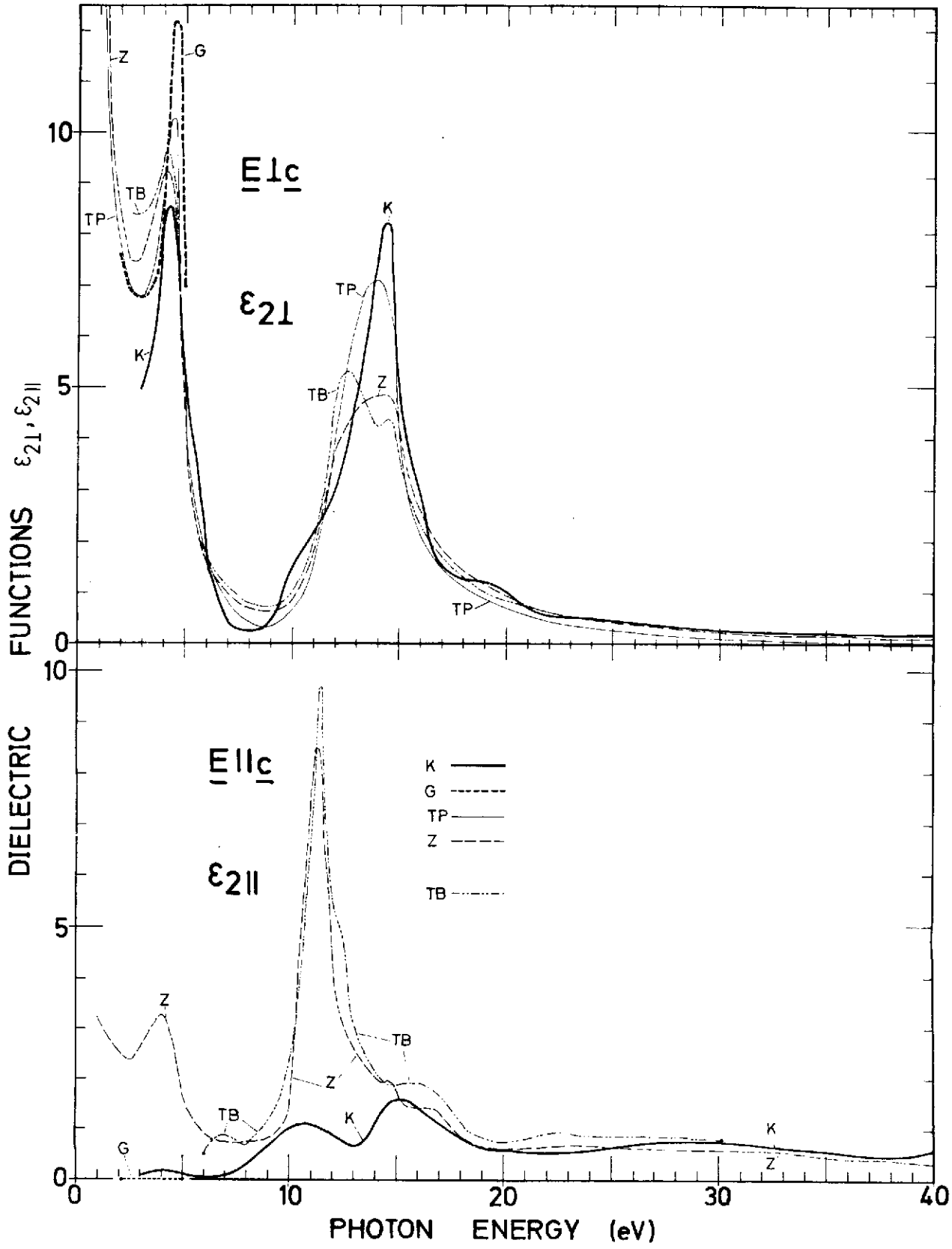
DIELECTRIC FUNCTIONS $\varepsilon_{2\perp}, \varepsilon_{2\parallel}$
$E \perp c$
$\varepsilon_{2\perp}$
$E \parallel c$
$\varepsilon_{2\parallel}$
K
G
TP
Z
TB
PHOTON ENERGY (eV)
0
5
10
20
30
40

Fig. 6

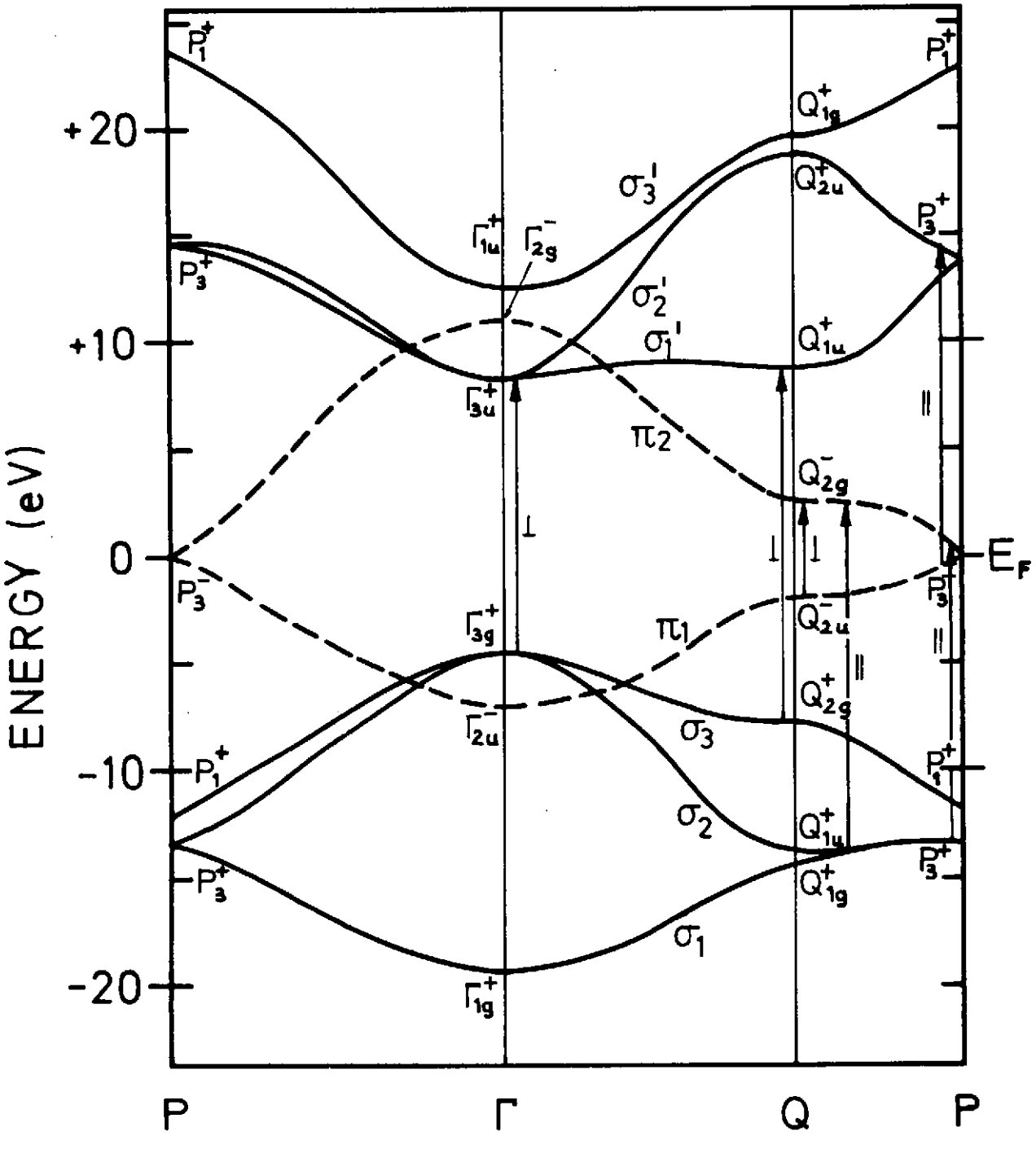
ENERGY (eV)
+20
+10
0
-10
-20
P
Γ
Q
P
E_F
P_1^+
P_3^+
P_3^-
Γ_{1u}^+
Γ_{2g}^-
Γ_{3u}^+
Γ_{3g}^+
Γ_{2u}^-
Γ_{1g}^+
Q_{1g}^+
Q_{2u}^+
Q_{1u}^+
Q_{2g}^-
Q_{2u}^-
Q_{2g}^+
Q_{1u}^+
Q_{1g}^+
σ_3'
σ_2'
σ_1'
π_2
π_1
σ_3
σ_2
σ_1
⊥
∥

Fig. 7

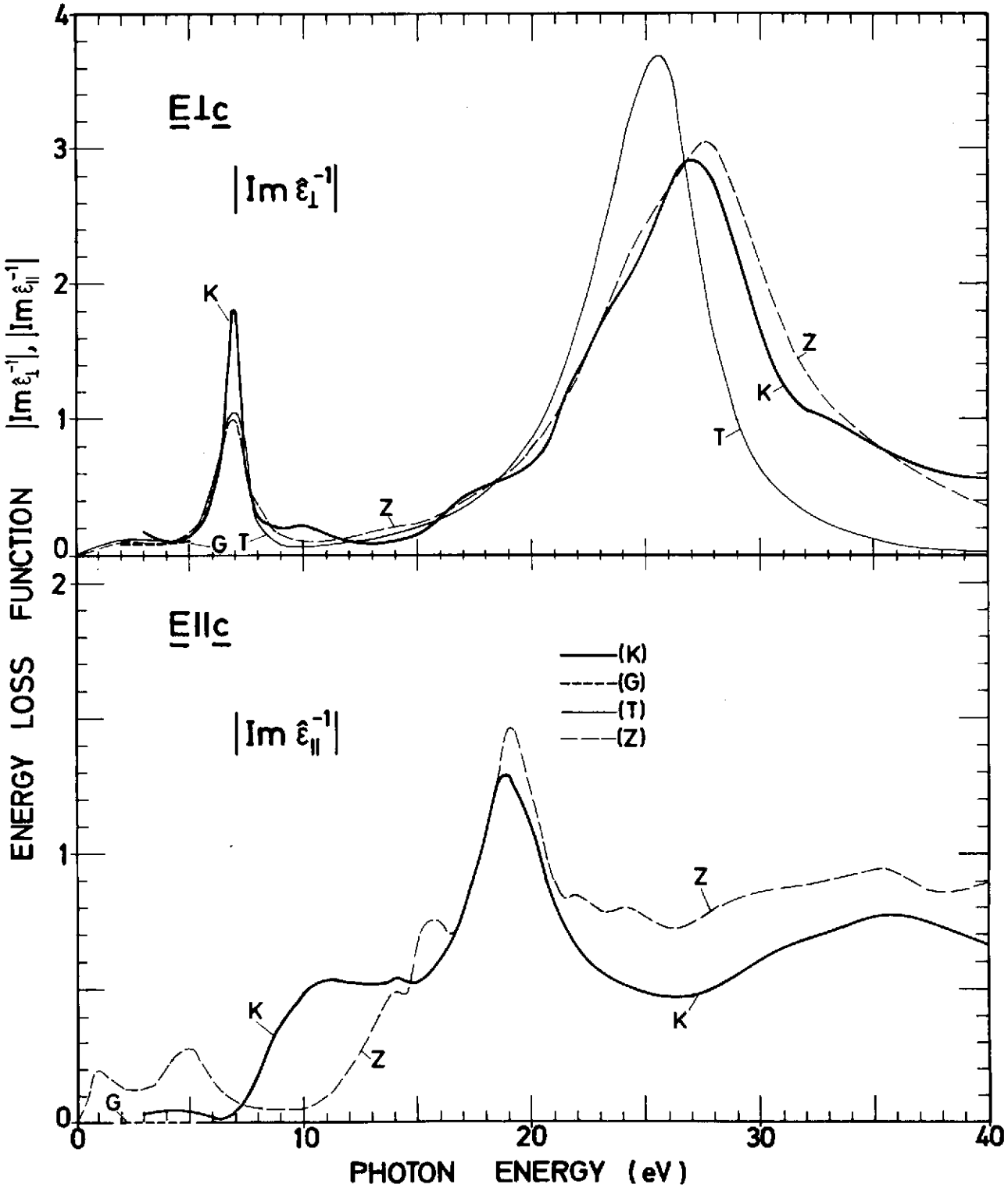
E⊥c
$|\mathrm{Im}\,\hat{\varepsilon}_{\perp}^{-1}|$
K
Z
K
T
G
T
Z
E∥c
$|\mathrm{Im}\,\hat{\varepsilon}_{\parallel}^{-1}|$
(K)
(G)
(T)
(Z)
Z
K
K
Z
G
ENERGY LOSS FUNCTION $|\mathrm{Im}\,\hat{\varepsilon}_{\perp}^{-1}|, |\mathrm{Im}\,\hat{\varepsilon}_{\parallel}^{-1}|$
PHOTON ENERGY (eV)
0
10
20
30
40
0
1
2
3
4
0
1
2

Fig. 8

$\varepsilon_2\omega^2$ (ARBITR.UNITS)
2
1
0
0
10
20
30
PHOTON ENERGY (eV)
(4.0)
4.5
5.5
7.0
10.5
11.0
14.8
15.0
16.0
20.0
28.5
29.0
E ⊥ c
E ∥ c

Fig. 9